Supporting Information

Efficient Electrocatalytic Water Oxidation by Fe(salen)–MOF Composite: Effect of modified microenvironment

Subhabrata Mukhopadhyay, Olivia Basu, Aranya Kar and Samar K. Das*

School of Chemistry, University of Hyderabad, Hyderabad – 500046, India

Table of Contents:

Section S1. Physical Measurements

The synthesized compounds were characterized by powder X-ray diffraction (PXRD), FT-IR, UV-Vis. diffused reflectance spectroscopy (DRS), Gas sorption analysis, FESEM-EDX, X-ray photoelectron spectroscopy, inductively coupled plasmon atomic emission spectroscopy (ICP-AES) and Electrochemistry.

Fourier transformed - Infrared spectra of solid samples were recorded on an iD7 ATR Thermo Fisher Scientific-Nicolet iS5 instrument. The powdered sample was directly put on the sample holder without any modification. Diffuse Reflectance (DRS) UV-Vis spectra were recorded using Shimadzu-2600 spectrophotometer. Field emission Scanning Electron Microscope (FE-SEM) imaging with energy dispersive X-ray (EDX) spectroscopy was carried out on a Carl Zeiss model Ultra 55 microscope: EDX spectra and maps were recorded using Oxford Instruments X-Max^N SDD (50 mm^2) system and INCA analysis software. All electrochemical experiments were conducted using a Zahner Zanium electrochemical work station operated with Thales software.

Section S2. Synthesis, Material and Synthetic procedures:

All the chemicals were received as reagent grade and used without any further purification.

Synthetic procedure is mentioned in the main manuscript.

Section S3. PXRD pattern of ZIF-8 and FSWZ-8:

PXRD patterns of **FSWZ-8** match well with the simulated pattern of ZIF-8. Though there were variation in the relative peak intensities of the composites prepared when compared with ZIF-8 but no notable shift was present in peak positions. It infers that, no appreciable change occurred in the crystal structure of ZIF-8 due to SiW_{12} and Fe-salen encapsulation.

Section S4. FT-IR spectral analysis of ZIF-8, Fe(salen)Cl and FSWZ-8:

For ZIF-8 the characteristic peaks appear at ~2920 cm^{-1} (ν 'C-H', aromatic), 1684 cm^{-1}(ν 'C=N'). Two broad bands ranging from 1384 cm^{-1} to 1506 cm^{-1} (imidazole ring stretch) and from 949 cm^{-1} to 1336 cm^{-1} (imidazole ring in-plane bending) can also be observed for the FT-IR spectrum of ZIF-8 (Figure S1).

However, all the composites mainly show FT-IR peaks similar to that of ZIF-8. This might be a result of masking of the low intense peaks of the guest molecules by peaks of the host species ZIF-8. Peaks due to the presence of Fe-salen were also observed in the FT-IR spectrum of **FSWZ-8** and marked in the plotted spectra (Figure S1)

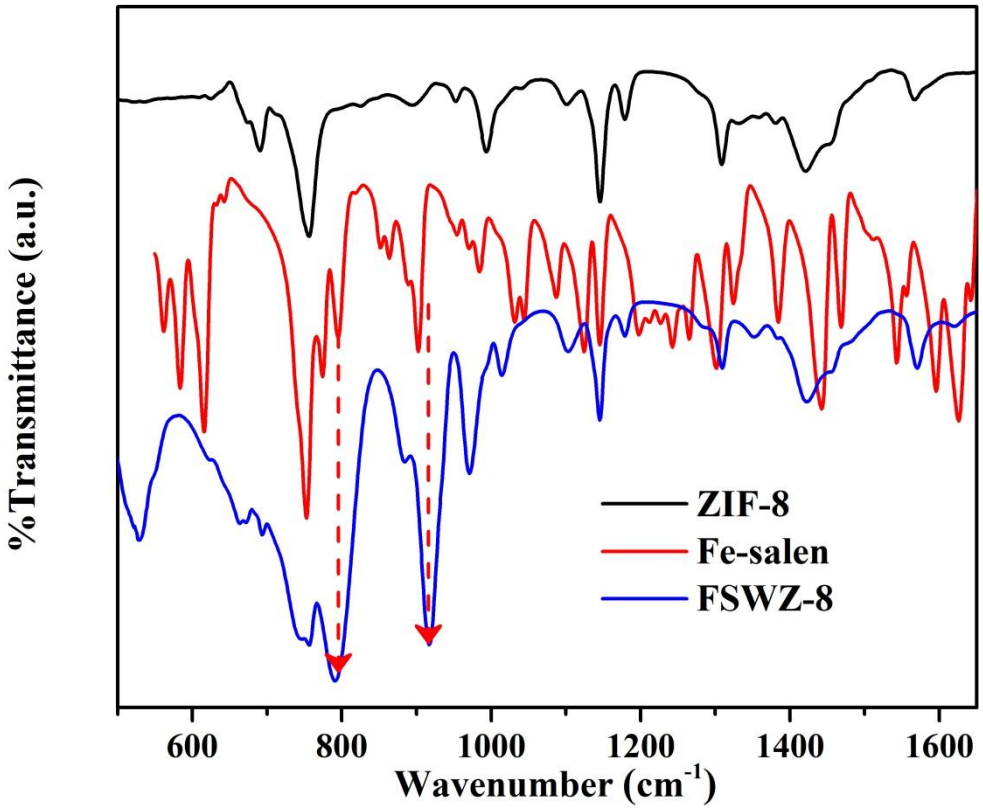

Figure S1. FT-IR spectra of ZIF-8, Fe(salen)Cl, **FSZ-8** and **FSWZ-8**.

Section S5. UV-Visible spectral analysis of ZIF-8, Fe(salen)Cl and FSWZ-8:

Solid state UV-Visible diffused reflectance (DR) spectra were recorded in wavelength-reflectance mode using $BaSO_4$ as the reference. All the spectra were Kubelka-munk converted into wavelength-absorbance mode for the sake of convenience and analysed. ZIF-8 has no prominent absorption feature in the visible region.

Section S6. Field Emission Scanning Electron Microscopy (FESEM) and Energy-dispersive X-ray (EDX) Analysis:

FESEM images of the **FSWZ-8**, **FSZ-8** were recorded. FESEM images of electrode coated materials were also recorded. A comparison of FESEM images of **FSZ-8** and **FSWZ-8** shows the relatively rough surface of **FSWZ-8** in comparison to **FSZ-8** due to the surface growth of SiW_{12} POM. The FESEM images of the sample coated carbon cloth electrodes after electrochemical analysis contains particles of hexagonal morphology, typically similar to the well-established hexagonal morphology of ZIF-8 particles. On the other hand, in the FESEM images of the carbon cloth electrode after the controlled electrochemical experiments of **FeO_x-CC** and **FeO_x-Z8** shows presence of spherical nano-particles, which is very common in case of metal oxide deposition on electrode surface.

Energy dispersive X-ray (EDX) spectroscopy was carried out for **FSWZ-8** (Figures S2 and S3) to check the surface composition of both the materials. Due to very low loading of Fe-salen the presence of iron on the surface is found to be negligible in all EDX analysis. On the other hand, much higher loading of SiW_{12} POM could also be verified by high surface concentration of tungsten. The growth of POM on the surface can also contribute to the high abundance of SiW_{12} found in the EDX measurements.

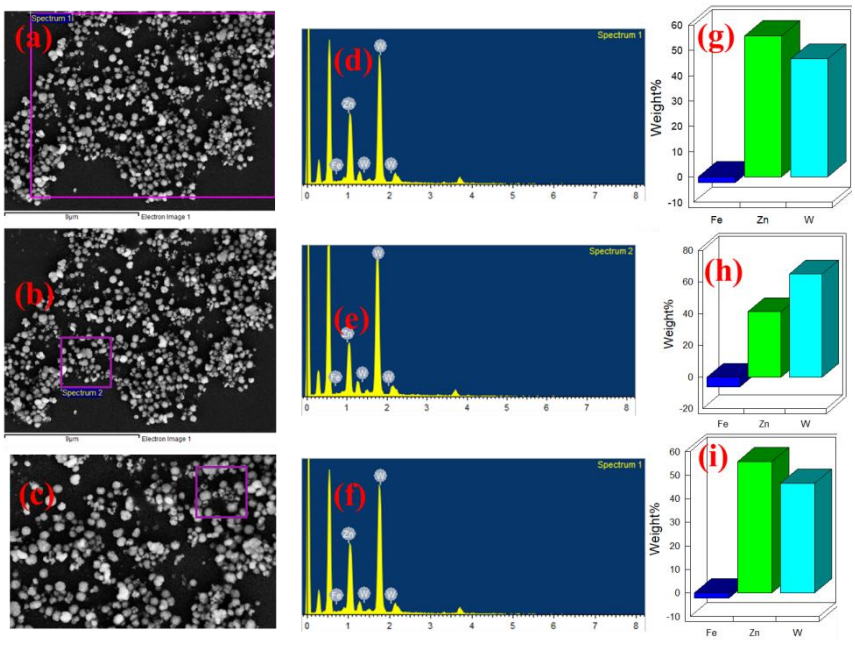

Figure S2. EDX analysis of different places on the surface of **FSWZ-8**. (a), (b), (c) images of surface of **FSWZ-8**, (d), (e), (f) experimentally recorded histogram of elemental composition; (g), (h), (i) EDX elemental analysis.

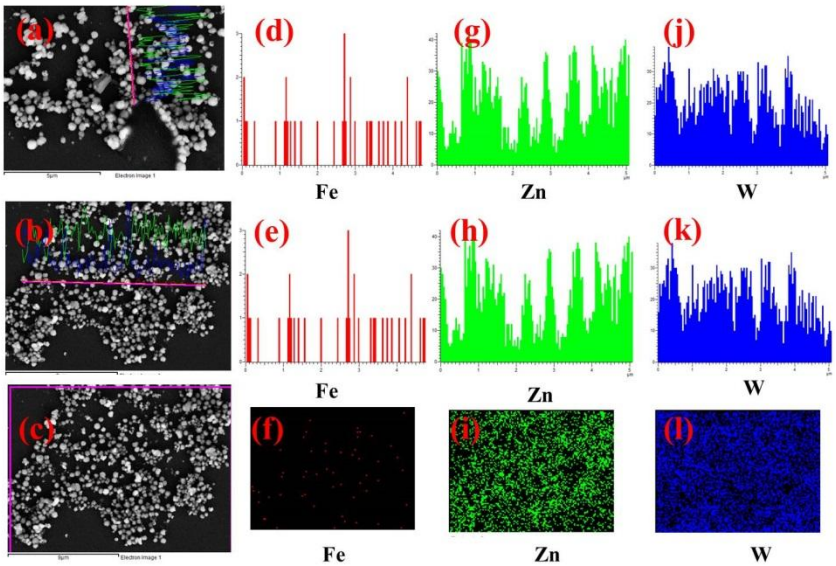

Figure S3. EDX elemental mapping and line scan of **FSWZ-8**. a), (b), (c) images of surface of **FSWZ-8**, (d)&(e), (g)&(h), (j)&(k) shows elemental composition of Fe, Zn and W during two different line scans. (f), (i), (l) shows elemental mapping of Fe, Zn and W on **FSWZ-8** surface.

Section S7. HRTEM analysis of FSWZ-8:

HRTEM analysis of the **FSWZ-8** and **FSZ-8** were carried out. Hexagonal particles of ZIF-8 were visible in both cases with spherical incorporated species, which might be either of the guest species *i.e.,* Fe-salen or SiW_{12} POM.

Section S8. Elemental analysis of FSZ-8 and FSWZ-8 from ICP-OES analysis and calculation of cell occupancy from weight percentage:

The elemental composition of **FSZ-8** and **FSWZ-8** were analysed and confirmed by Inductively Coupled Plasma Optical Emission Spectrometry (ICP-OES). From elemental analysis we found that level of loading of Fe-salen is much higher in **FSWZ-8** than **FSZ-8**. It suggests a loading of one Fe-salen unit in each 25 cages of ZIF-8 because a single cage of ZIF-8 consists of 12 ($C_8H_{10}N_4Zn$) units (*vide infra*). The loading level of SiW_{12} POM was also determined from the ICP-OES analysis. The loading level suggests that the POM has not only been encapsulated but has also grown on the surface of ZIF-8 by the in situ synthetic technique.

Calculation of unit cell occupancy by Fe-salen and SiW_{12} units:

The calculation is simplified by using **Zn**, **Fe** and **Si** as the representative of ($C_8H_{10}N_4Zn$), [Fe(salen)(OH)] and ($H_4[SiW_{12}O_{40}]$) unit.

Now, each unit cell of ZIF-8 consists of 24 ($C_8H_{10}N_4Zn$) units. 4 Zn ions situate on each face (total 6 faces) of the unit cell. Thus, each of the Zn is shared between two adjacent unit cells.

Therefore, contribution per Zn = ½.

Effective number of Zn in each unit cell = 24 × ½ =12

Thus, each unit cell has 12 ($C_8H_{10}N_4Zn$) units.

So, **in case of FSWZ-8 the unit cell occupancy of [Fe(salen)(OH)] should be approximately 2 Fe-salen unit per 25 cages of ZIF-8**.

However, **Zn**: **Si** ≈ 25:32 (from atomic ratio)

It is highly improbable for 25 ZIF-8 cages to incorporate 32 SiW_{12} POM units. Thus, the ICP-OES results strongly suggest the growth of SiW_{12} POM on the ZIF-8 surface along with its encapsulation in the cavities. This is also supported by the surface roughening of **FSWZ-8** due to SiW_{12} growth on the surface which is explained in details in the main manuscript.

The ICP-OES analysis also suggests a very low loading of Fe-salen species (<0.01 %) in case of **FSZ-8**, which indirectly proves the assistive role played by the SiW_{12} Keggin for the encapsulation of Fe-salen in case of **FSWZ-8**.

ICP-OES Test report for FSWZ-8 and FSZ-8:

Issued to:
Prof Samar K.Das
School Of Chemistry
University of Hyderabad, Gachibowli,
Hyderabad-500046
Kind Attn.:Subhabrata Mukhopadhyay,
Sample Particulars : **FSWZ-8 & FSZ-8**

Report No. : LL/19-20/003964 - 003965
Issue Date : 25/07/2019
Customer Ref. TRF
Ref.Date : 20/07/2019

Sample Qty.: 2nos, Vial
Test Required : Iron as Fe,Silicon as Si,Zinc as Zn
Date of Receipt of Sample : 23/07/2019
Date of Starting of Analysis : 25/07/2019
Date of completion of analysis : 25/07/2019
SAMPLE TESTED AS RECEIVED

TEST RESULTS

S.No.	Regn.No.	Sample ID	Iron as Fe % by mass	Silicon as Si % by mass	Zinc as Zn % by mass
1	LL/19-20/003964	FSWZ-8	0.069	0.55	11.12
2	LL/19-20/003965	FSZ-8	<0.01	---	34.20

Instrument Used: ICP-OES Varian 720-ES
NOTE : This report and results relate only to the sample / items tested.
Note: The above results are only for infrmation purpose not for any regulatory submission

Section S9. Gas (N_2) sorption analysis of FSWZ-8 and ZIF-8:

N_2 sorption measurement has been carried out for ZIF-8 and **FSWZ-8** to understand the surface area and porosity of **FSWZ-8**. Prior to Gas sorption measurement both the compounds were degassed for 10 hours in 120 °C temperature. Available surface area for N_2 sorption was calculated using Brunauer–Emmett–Teller (BET) method from the mono-layer portion of the sorption isotherm. BET surface area was found to be 746 m^2g^{-1} and 1403 m^2g^{-1} for ZIF-8 and **FSWZ-8** respectively.

Section S10. X-Ray photoelectron spectroscopy:

The X-Ray Photoelectron Spectroscopy (XPS) of the samples were recorded on a Thermo Scientific NEXSA photoemission spectrometer using Al-K_α (1486.6 eV) X-ray radiation. The raw data obtained from the instrument was then deconvoluted and fitted with the help of Avantage software.

The XPS data for Fe-salen and **FSWZ-8** were recorded (Figure S4), for which the samples were sonicated in water and MeOH respectively for 5 minutes and drop casting was done on Si wafer. XPS survey for Fe-salen confirms the presence of Fe, C, N, O and Cl (Figure S4a) and that of **FSWZ-8** confirms the presence of Zn, Fe, O, N, C, Si, W and Cl (Figure S4b). Deconvolution of Fe2p scan for Fe-salen showed peaks for Fe^{3+} (710.8, 723.8) and Fe^{3+} satellites (717.9, 730.1 eV), in addition to that two peaks at 714.26 and 726.4 eV can be

assigned to Fe^{2+} satellites. On the other hand, the deconvoluted Fe2p scan for Fe-salen-POM@ZIF-8, showed lot of shifting in the binding energy (B.E.), which could be due to insulating nature of ZIF-8 (Figure S4c). Repetitive measurement also provided with similar data of huge XP spectral shift. Thus we assumed the electrical resistive nature of ZIF-8 to cause a charge accumulation at the surface of ZIF-8 under analysis, which may further affect the immediate adjacent layers beneath the surface by a dipole interaction.

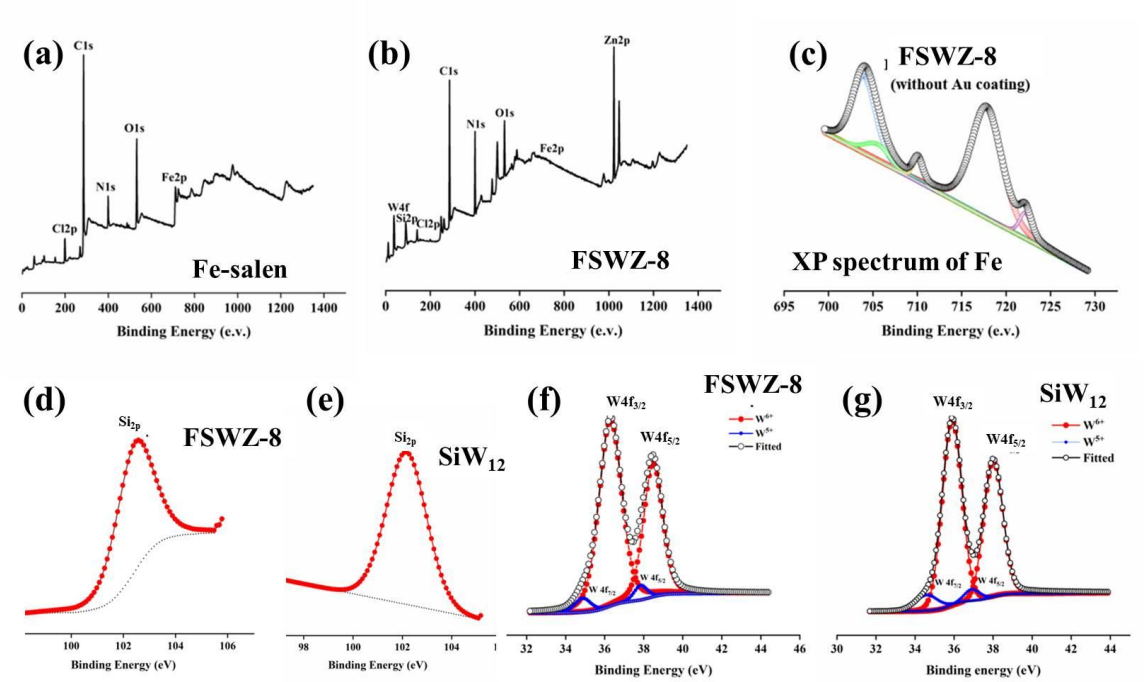

Figure S4. (a), (b) XPS survey of surface of Fe-salen and **FSWZ-8**. (c) XP spectrum of Fe of **FSWZ-8,** without Au coat. (d), (e) Fitted Si_{2p} XPS of **FSWZ-8** and SiW_{12} POM respectively. (f), (g) Fitted and deconvulated W XPS of **FSWZ-8** and SiW_{12} POM.

To nullify any issues arising due to the insulating factor of ZIF-8, we first sonicated the sample in MeOH and prepared a very thin layer of coat on Si wafer by dipping it into the solution. After drying the Si wafer overnight, we coated it with 2 nm layer of Au, to increase the conductivity of the material. XPS survey for the gold coated sample showed the presence of W, Si, Au, Fe, C, N. Deconvolution of Fe2p scan for this Au coated revealed five peaks, which can be assigned to Fe^{3+} (710.8, 724 eV), Fe^{3+} satellites (718, 730.8 eV) and one Fe^{2+} satellite (714.24 eV).

From the gold coated **FSWZ-8** material, we observed a prominent but realistic shift in Fe^{3+} XP spectra when compared to Fe-salen. Minor shifts were also observed in the W4f spectrum of **FSWZ-8** when compared to that of SiW_{12} POM. This indicates electronic interaction to take place between ZIF-8 cavity and both the guest species *i.e.*, Fe-salen and SiW_{12} POM.

Section S11. Electrochemical analysis:

All electrochemical experiments were performed using a three-electrode electrochemical cell employing glassy carbon as working, Ag/AgCl (1M) as reference and Pt-wire as counter electrodes in a heterogeneous way.

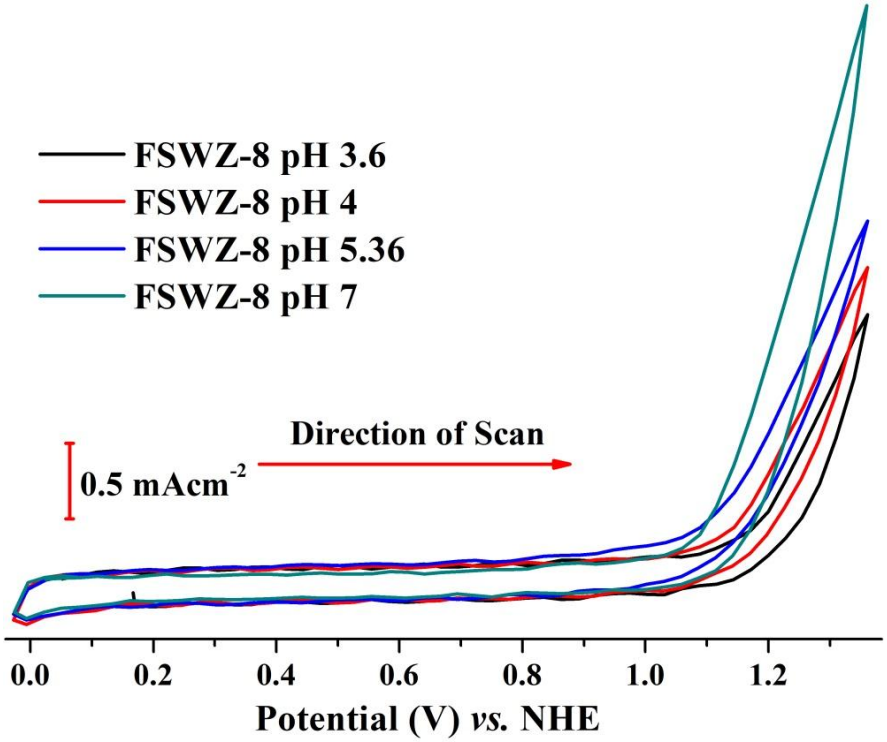

Figure S5. Cyclic voltammogram of **FSWZ-8** in aqueous solution of different pH (from acidic to neutral). Used electrolyte was 0.1 M KCl. 0.1 M HCl was used to maintain pH.

Tafel Data Collection

Tafel data was collected in galvanostatic mode. For this constant current was applied for 15 minutes. After 15 min the steady state potential was noted. Likewise different currents were applied within the range of 10^{-5} A to 10^{-3} A. The electrolyte solution was stirred at 450 rpm throughout the experiment to maintain steady state mass flow to the electrode. Before starting the measurement, the solution resistance was directly read out from instrument iR function. This resistance value was used to correct the uncompensated resistance manually for each current value.

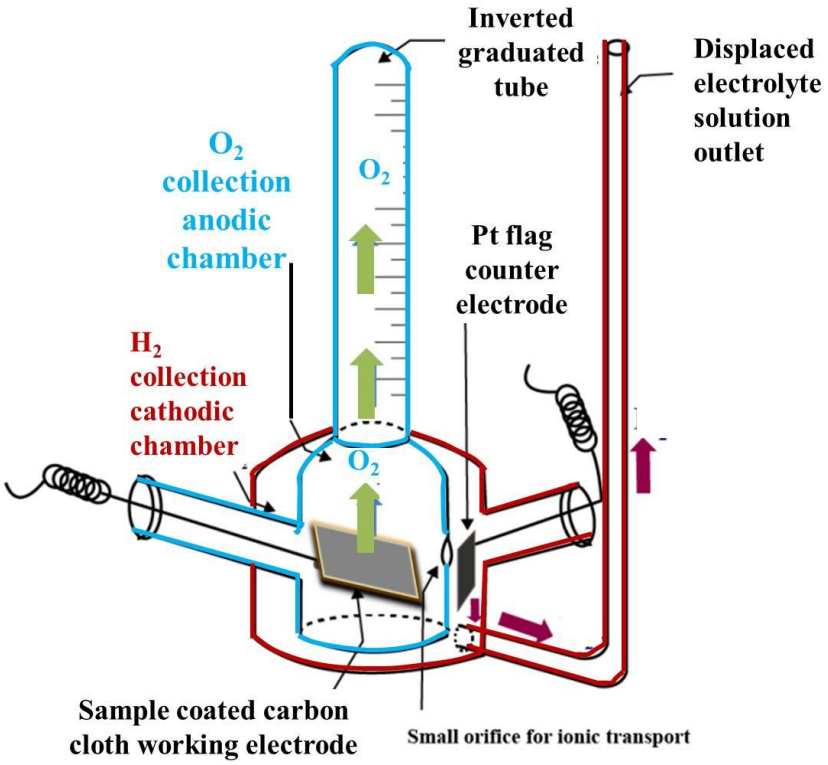

Figure S6. Schematic of the home-made quantitative gas determination set up used to calculate Faradic efficiency of **FSWZ-8.**

Section S12. Quantitative oxygen evolution experiment and calculation of Faradic efficiency:

To determine the evolved oxygen (O_2) gas over time, bulk electrolysis was carried out at constant current using a two electrode systems for **FSWZ-8**. Sample coated carbon cloth electrode was used as the working electrode (anode) and a large area platinum flag was used as counter electrode (functions as cathode). Known amount of catalyst was loaded on the carbon cloth working electrode. 0.1 M KCl was used as the electrolyte. Using a home built set up, which can separate the evolved O_2 and H_2 generated during OER at the working electrode and counter electrode respectively and also can measure the volume of O_2 generated from the working electrode with a precession of 0.05 mL, electrolysis was carried out (Figure S6). A constant current density of 1 $mAcm^{-2}$ was applied in each case for a period of 8 h. During the electrolysis, oxygen bubbles evolved from the surface of the carbon cloth electrode accumulates in an inverted graduated tube fixed on the top of the working electrode chamber. The chamber initially stays filled with electrolyte solution but as the experiment proceeds and more oxygen is generated, the oxygen displaces the electrolyte solution and occupies the place by solvent (in this case electrolyte solution) displacement method. As we have already mentioned that this inverted tube is graduated. Thus, the evolved amount of oxygen can be quantified. On the other hand, the H_2 gas generated from the counter electrode gathers on the top of the counter electrode chamber and forms a ring of bubble around the inverted graduated tube of working electrode chamber. But it cannot get inside the tube and mix up with O_2. The set up was constructed such that, no gas evolved in the cathode chamber could enter into the

anodic chamber. It is important to mention that, to maintain electrical connectivity, the glass tube functioning as the barricade between the anodic/working electrode chamber and cathodic/ counter electrode chamber was not sealed at the bottom and a small window was kept between the working and counter electrode. This arrangement is crucial to maintain the electro neutrality and continue the measurement for prolonged period.

Faradic efficiency:

From the quantitative measurement of evolved oxygen in bulk electrolysis under constant current condition, 0.40 mL/hour of O_2 evolution was observed under 1 atm. Pressure.

Thus, moles of O_2 evolved in one hour = (0.40/22400) mol = 17.8 μmol.

Therefore Faradaic efficiency of **FSWZ-8** was calculated to be 95.44 %.

Section S13. TOF Calculation:

The activity of a catalyst can be conveniently defined in terms of turnover frequency (TOF). The number of reactant molecules getting converted into product molecules in unit time per active site is called the TOF of a catalyst for a particular process. The TOF is measured as given in the literature.[2]

$$\text{TOF at any given over potential} = \frac{\text{Current density at given over potential}}{4 \times F \times \text{No. of Fe(salen)(OH)}} \quad \text{....(1)}$$

Here, 4 is used because OER is a $4e^-$ process. Hence division of current density at a particular overpotential by 4F (F = Faraday constant) gives one catalytic turnover number and further division of this turnover number by the number of active Fe-salen species results in turnover frequency (TOF).

In this case, the complete coated sample on electrode was assumed to be electrochemically active towards OER to avoid any ambiguity for TOF calculation. The reason behind such approximation was (a) difficulty to determine the exact electrochemically active surface area of **FSWZ-8** because of probable access of internal surface to some extent; (b) difficulties to determine the *surface coverage by active species* due to lack of prominent reversible redox couple in the cyclic voltammogram of **FSWZ-8**. Thus the TOF reported here actually represents the lower limit of the TOF of the material, which may (most probably!) have much higher value because it is highly unlikely that the whole coated bulk sample can be active towards OER at any instance.

Calculation:

The total amount of coated sample was 10 μL.

The sample ink was prepared by mixing 2 mg of acetylene carbon black and 8 mg of sample in 2 mL of ethanol water mixture (ethanol : water = 2:1). Considering the ink to be homogeneous in nature, a 10 μL of coated material should have 40 μg of sample in it.

Now, molecular weight of **FSWZ-8** is ≈ 161162.

So, 40 μg of sample of **FSWZ-8** contains 0.5 nmol. of **FSWZ-8**.

Thus, $TOF_{j=1\ mA/cm^{-2}} = [10^{-3}/(4\times96500\times5\times10^{-10})]$

$\mathbf{(TOF)_{j=1\ mA/cm^{-2}}} \approx \mathbf{5.2}$ [(mol. O_2)(mol. Fe)$^{-1}$s^{-1}]

Section S14. Impedance measurement and analysis:

Electrochemical impedance spectroscopy (EIS) was performed on both the compounds *i.e.*, **FSZ-8** and **FSWZ-8** to have further insight about the mechanism involved. The impedance measurements were performed in a three electrode set up using sample modified glassy carbon as working electrode, Ag-AgCl as the reference electrode and Pt-mesh as the counter electrode under 1.2 V anodic potential, which is actually, the potential of catalytic OER performed by both the catalysts. Nyquist and Bode plots were recorded within the frequency region of 1 Hz to 1×10^6 Hz.

Section S15. Characterization of electrode coated sample and electrolyte after electrochemical analysis:

To understand the stability of **FSWZ-8** as OER catalyst, PXRD and FESEM imaging were done with the sample coated carbon cloth electrode (before and after electrochemical analysis). ICP-OES was performed on the electrolyte after bulk electrolysis to check the leaching due to structural degradation.

To perform the 6 hours chronoamperometric measurements the coating on carbon cloth electrode was prepared by drop casting of sample ink over carbon cloth working electrode and drying under IR lamp. The sample ink was prepared by sonication of 2 mL suspension prepared by mixing sample and carbon black in the ration of 10:1. As the carbon cloth electrode contains highly conducting carbon fibres and can come in more intimate contact with the sample than glassy carbon electrode, thus the opportunity to lower the carbon content from the sample mixture was exploited. This lower concentration of acetylene carbon black was beneficial for performing the PXRD and FESEM analysis of the electrode and compare. Further characterization of the electrolyte after bulk electrolysis was carried out by ICP-OES analysis of any probable product by leaching of Fe-species.

From the PXRD analysis (Figure S7), no notable change could be found in the crystal structure of ZIF-8, which shows the robustness of the ZIF-8 framework under operational conditions. No spherical metal oxide nano-particle could be detected from the FESEM images of the same electrode. These two post-chronoamperometric treatment indicates towards the high stability of the material. Besides, the ICP-OES analysis of the electrolyte also shows no appreciable leaching of any iron species in the electrolyte which also indicates the same.

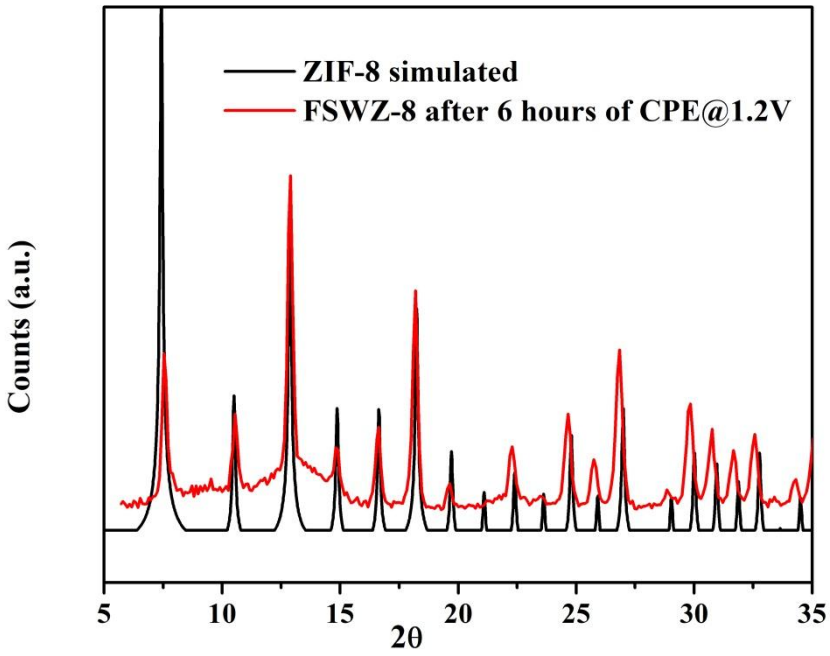

Figure S7. Comparison of PXRD pattern of **FSWZ-8** after 6 hours of chronoamperometry in 0.1 M KCl compared with simulated pattern of ZIF-8.

ICP-OES analysis of electrolyte after accelerated durability test:

No trace of Fe or W could be found in the electrolyte solution after 6 hours of chronoamperometric analysis by ICP-OES analysis. This proves no notable leaching of either of the guest species from the cavity of ZIF-8 in case of **FSWZ-8**. The ICP-OES reports are attached below.

ICP-OES analysis of electrolyte of FSWZ-8:

TEST REPORT

Name & Address of the customer:
Subhabrata Mukhopadhyay Research Scholar;
C/o Prof. Samar Kumar Das
School of Chemistry

Test Report No : 577
Issue Date : 22-05-2019
Sample Reg. No : 1405031542
Received on : 14-05-2019
Sample condition at receipt : Found Ok
Test Commenced on : 15-05-2019
Test Completed on : 21-5-2019

Sample Particulars: Liquid Sample
Sample quantity : 8 ml pack
Packing : Packed in plastic bottles
Test required : Fe, Zn, W

Test Results

Analysis results in %

S. No	Name of Sample	Elements analyzed		
		Fe	Zn	W
1.	Electrolyte of FSWZ-8	----	-----	-----

Section S16. Spectroscopic analysis and controlled experiments to understand the true catalytic nature of FSZ-8 and FSWZ-8 towards electrochemical OER:

To understand and analyze the structural integrity of the encapsulated Fe-salen species, controlled experiments and spectroscopic analysis were performed by UV-Visible DRS spectroscopy, Raman and FT-IR spectroscopy. Furthermore, electrochemical experiments were also performed.

UV-Visible spectra of Fe(salen)Cl and **FSWZ-8**, recorded in DRS mode, shows similar features with notable shift. Of note, no characteristic feature of SiW_{12} POM could be observed in the UV-visible spectrum of FSWZ-8, as SiW_{12} has less prominent absorption within the measured wavelength region.

In case of the FT-IR spectroscopic analysis, the FT-IR spectrum of **FSWZ-8** is mostly similar to that of ZIF-8, which may be a consequence of very low loading of Fe-salen species inside ZIF-8 cavity. However, a detailed comparison shows, few peaks of ZIF-8 were shifted from their original positions in **FSWZ-8** (*vide supra*).

Finally, Raman spectral analysis of Fe(salen)Cl and **FSWZ-8** (Figure S8a) were carried out using a 786 nm laser. The Raman spectrum of **FSWZ-8** is observed to have excellent similarity with that of synthesized Fe(salen)Cl coordination complex. Little spectral shifts are common for most of the Raman stretches of **FSWZ-8** compared to those of Fe(salen)Cl.

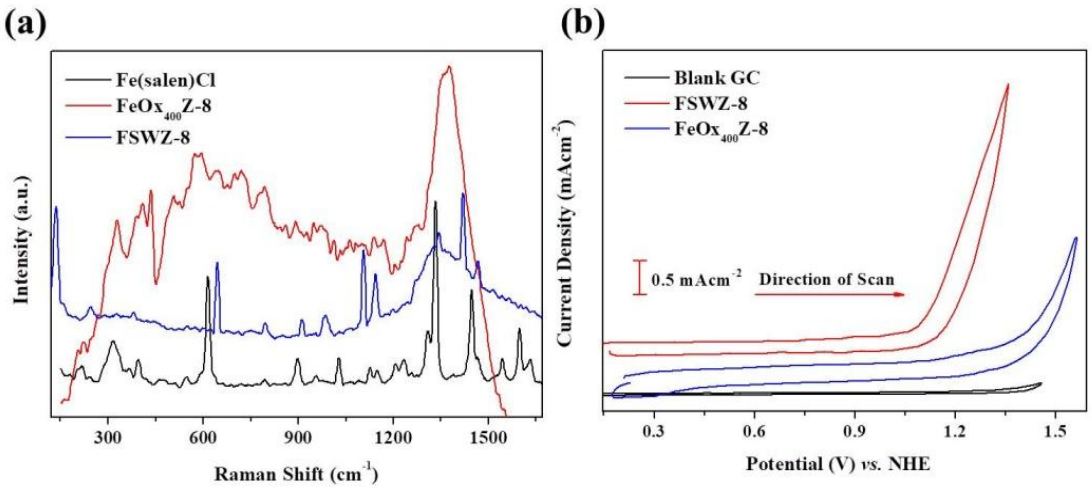

Figure S8. (a) Raman spectra of **FSWZ-8**, Fe(salen)Cl and **$FeOx_{400}$Z-8** (Fe-salen@ZIF-8 thermally treated at 400°C) recorded using 786 nm laser. **(b)** Cyclic voltammograms of blank glassy carbon electrode (GC), **FSWZ-8** and **$FeOx_{400}$Z-8**.

All these spectroscopic analyses indicate that, the basic structure of the Fe-salen species remains unchanged inside the ZIF-8 cavity. However, the encapsulation process accompanies with some electronic redistribution between the host ZIF-8 and guest Fe-salen species that can result in the spectral shifts in the UV-Visible, FT-IR and Raman spectra of **FSWZ-8**.

To analyze any chances of partial or complete conversion of the Fe-salen species into iron oxide inside the cavity of ZIF-8 during encapsulation process or electrochemical measurements, **$FeOx_{400}$Z-8** was prepared following a protocol, reported by Zhang and coworkers[3] and subjected to electrochemical measurements. The **$FeOx_{400}$Z-8** can be assumed as the closest iron-oxide containing sister compound of **FSWZ-8** that can account for the fact that the oxidative degradation of the Fe-salen inside the ZIF-8 cavity does not occur, either during the encapsulation or during electrochemical analysis. The synthesis of **$FeOx_{400}$Z-8** involves a two-step process *i.e.*, (1) encapsulation of the Fe(salen)Cl species inside ZIF-8 cavity following previously mentioned synthetic protocol and (2) thermal treatment of the newly formed composite material at 400°C for 3 hours. The temperature was set at 400°C because, it does not completely destroy the ZIF-8 framework but oxidizes Fe-salen species to iron oxide. Thus, we could prepare a **$FeOx_{400}$Z-8** composite which has tiny iron-oxide particles inside the ZIF-8 cavity.

Electrochemical measurements were carried out on the **$FeOx_{400}$Z-8** under similar experimental condition. As indicated by the cyclic voltammograms of **$FeOx_{400}$Z-8** (Figure S8 b and Figure S9 a), it shows a distinctly different electrochemical behaviour than that showed by **FSWZ-8** and also it requires higher potential to carry out electrochemical OER. The cyclic voltammetric features of **FSWZ-8** and **$FeOx_{400}$Z-8** were found to be distinctly different in neutral pH under similar operational conditions. Moreover, the choronoamperometric measurement (Figure S9b) of **$FeOx_{400}$Z-8** at 1.2 V shows the **$FeOx_{400}$Z-8** to be unstable under operational electrochemical conditions.

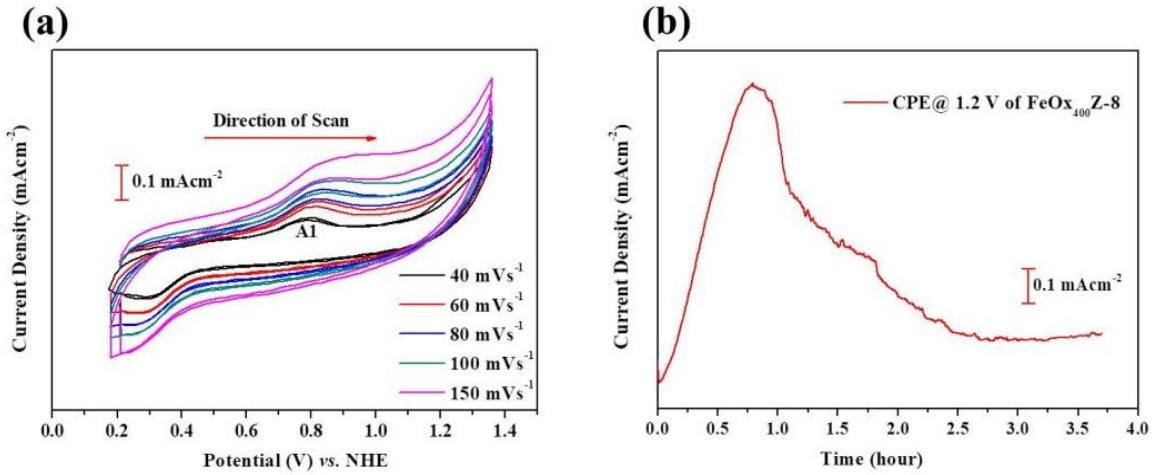

Figure S9. (a) Cyclic voltammograms of **$FeOx_{400}$Z-8** modified glassy carbon electrode at different scan rates in 0.1 M KCl. **(b)** Chronoamperometric analysis of **$FeOx_{400}$Z-8** at 1.2 V.

With all these controlled experiments, it can be inferred that, the Fe-salen species is stable inside the ZIF-8 cavity and does not convert to tiny iron oxide particles inside ZIF-8 cavity during or before the encapsulation process.

Furthermore, in order to comprehend, whether the activity towards electrochemical OER from **FSWZ-8** might be a result of *in situ* deposited FeO_x during the electrochemical analysis, control experiments were performed on FeO_x, deposited on the carbon cloth electrode (here after referred as **FeO_x-CC**) and also on FeO_x, deposited on ZIF-8 surface (here after referred as **FeO_x-Z8**). Under basic pH, electrodeposition of FeO_x onto carbon cloth (working electrode) surface was done by performing chronoamperometric analysis at 1.6 V for a period of 5 hours using carbon cloth as the working electrode, platinum flag electrode as counter electrode and Pt wire as pseudo reference electrode. After bulk electrolysis, a layer of FeO_x was deposited on the electrode surface. The coated layer was thoroughly washed and dried under IR-lamp to prepare a FeO_x layer on carbon cloth electrode. Similar method of coating of FeO_x was used to prepare layers of FeO_x on the surface of ZIF-8, which was already coated on carbon cloth electrode. Initially, sample ink of ZIF-8 was coated on carbon cloth electrode and dried under IR lamp. Then the modified electrode was employed for the bulk electrolysis using similar protocol, performed earlier to coat FeO_x on ZIF-8.

With the modified electrodes, thus prepared, *i.e.,* **FeO_x-CC** and **FeO_x-Z8**, the following electrochemical experiments were conducted: (1) cyclic voltammetry, (2) galvanostatic measurements to construct of Tafel plots and (3) chronoamperometric measurement at 1.3 V. Following the chronoamperometric measurement, the electrodes were also analysed by FESEM and EDX analysis.

The cyclic voltammetry features of the **FeO_x-CC** and **FeO_x-Z8** were observed to be widely different from that of **FSWZ-8**. The oxide materials did not show appreciable OER current within the potential window of our interest. This provides a very strong argument against any probable participation by *in situ* generated FeO_x in the electrochemical OER activity of the **FSWZ-8**. Further support to the same theory was provided by the Tafel plots of both the oxide materials. They were observed to have higher overpotential requirement than that required by **FSWZ-8**. FESEM images of the oxide coated electrodes were recorded after

chronoamperometric measurement at 1.3 V (*vs.* NHE) for 6 hours. In the FESEM images of the electrodes, the surfaces were observed to be covered by spherical metal oxide *i.e.*, FeO_x particles unlike the **FSWZ-8** electrode after chronoamperometric measurement.
Thus, with the help of all these electrochemical analysis and controlled experiments, the true catalytic nature of **FSWZ-8** could be proved in an indirect manner.

Table S1. Previous reports of MOF based electrochemical OER catalysts

Code name	Overpotential [η] (mV)	TOF ($\times 10^{-2}$ s^{-1})	Electrode	Electrolyte and pH	Reference
FSWZ-8	**516 (1 mA cm^{-2})**	**523 (η = 516 mV)**	**GC**	**0.1 M KCl (7)**	**Present work**
Co-ZIF-9	510 (1 mA cm^{-2})	0.058 (η = 300 mV)	FTO	0.1 M KOH (13.4)	4
FeTPyP-Co	351 (1 mA cm^{-2})	1220 (η = 310 mV)	GC	0.1 M NaOH (13)	5
Co-WOC-1	390 (1 mA cm^{-2})	5 (η = 390 mV)	GC	0.1 M KOH (13)	6
Fe3-Co2@GC	431 (2 mA cm^{-2})	13.2 (η = 400 mV)	GC	0.1 M PB (7)	7
UiO-67-[RuOH2]	818 (0.15 mA cm^{-2})	0.046 (η = 400 mV)	FTO	1 M KNO3 (6.2)	8
$[Co(bpy)(fa)]_n(DMF)_{0.25}(bpy)_{0.25}$	382 (10 mA cm^{-2})	0.2 (η = 289 mV)	FTO	0.1 M PB (7)	9
CoHCF	460 (0.1 mA cm^{-2})	50 (η = 550 mV)	FTO	50 mM PB, 1M KNO3 as a supporting electrolyte (7)	10
$\{[Co_3(pyz)(fa)_3(dmso)_2].2H_2O\}_n$	257 (1 mA cm^{-2})	0.2 (η = 261 mV)	FTO	PB, KNO3 as a supporting electrolyte (7.4)	11
Co-AIM NU-1000	566 (10 mA cm^{-2})	140 (η = 400 mV)	FTO	0.05 M NaHCO3 and 0.1 M NaOH (11)	12

References.

1. Bose, S.; Debgupta, J.; Ramsundar, R. M.; Das, S. K. Electrochemical Water Oxidation Catalyzed by an In Situ generated α-$Co(OH)_2$ Film on Zeolite-Y Surface. *Chem. Eur.J.* **2017**, *23*, 8051 –8057

2. Bediako, D. K.; Surendranath, Y.; Nocera, D. G. Mechanistic Studies of the Oxygen Evolution Reaction Mediated by a Nickel–Borate Thin Film Electrocatalyst *J. Am. Chem. Soc.* **2013**, *135***,** 3662-3674.

3. Mirza, S.; Chen, H.; Chen, S. M.; Gu, Z. G.; Zhang, J. Insight into Fe(Salen) Encapsulated Co-Porphyrin Framework Derived Thin Film for Efficient Oxygen Evolution Reaction. *Cryst. Growth Des.* **2018**, *18*, 7150–7157.

4. Liao, P-Q.; Shen, J-Q.; Zhang, J-P. Metal–organic frameworks for electrocatalysis. *Coord. Chem. Rev.* **2018**, *373*, 22–48.

5. Wurster, B.; Grumelli, D.; Hötger, D.; Gutzler, R.; Kern, K. Driving the Oxygen Evolution Reaction by Nonlinear Cooperativity in Bimetallic Coordination Catalysts. *J. Am. Chem. Soc.* **2016**, *138*, 3623–3626.

6. Manna, P.; Debgupta, J.; Bose, S.; Das, S. K. A Mononuclear Co^{II} Coordination Complex Locked in a Confined Space and Acting as an Electrochemical Water- Oxidation Catalyst: A "Ship- in- a- Bottle" Approach. *Angew. Chem. Int. Ed.* **2016**, *55*, 2425–2430.

7. Shen, J.-Q.; Liao, P.-Q.; Zhou, D.-D.; He, C.-T.; Wu, J.-X.; Zhang, W.-X.; Zhang, J.-P.; Chen, X.-M. Modular and Stepwise Synthesis of a Hybrid Metal−Organic Framework for Efficient Electrocatalytic Oxygen Evolution. *J. Am. Chem. Soc.* **2017**, *139*, 1778–1781.

8. Johnson, B.A.; Bhunia, A.; Ott, S. Electrocatalytic water oxidation by a molecular catalyst incorporated into a metal–organic framework thin film. *Dalton Trans*. **2017**, *46*, 1382–1388.

9. Batool, M.; Ibrahim, S.; Iqbal, B.; Ali, S.; Badshah, A.; Abbas, S.; Turner, D.R.; Nadeem, M.A. Novel cobalt-fumarate framework as a robust and efficient electrocatalyst for water oxidation at neutral pH. *Electrochim. Acta.* **2019**, *298*, 248–253.

10. Pintado, S.; Goberna-Ferrón, S.; Escudero-Adán, E.C.; Galán-Mascarós, J.R. Fast and persistent electrocatalytic water oxidation by Co-Fe Prussian blue coordination polymers. *J. Am. Chem. Soc.* **2013**, *135*, 13270–13273.

11. Ibrahim, S.; Shehzadi, K.; Iqbal, B.; Abbas, S.; Turner, D.R.; Nadeem, M.A. A trinuclear cobalt-based coordination polymer as an efficient oxygen evolution electrocatalyst at neutral pH. *J. Colloid Interface Sci.* **2019**, *545*, 269–275.

12. Kung, C.-W.; Mondloch, J.E.; Wang, T.C.; Bury, W.; Hoffeditz, W.; Klahr, B.M.; Klet, R.C.; Pellin, M.J.; Farha, O.K.; Hupp, J.T. Metal–organic framework thin films as platforms for atomic layer deposition of cobalt ions to enable electrocatalytic water oxidation. *ACS Appl. Mater. Interfaces* **2015**, 7, 28223–28230.

****